REMOTE SENSING OF DRYLANDS:
when soils come into the picture[1]

Richard Escadafal[2]

ABSTRACT

Among the striking features specific to drylands is the discontinuous vegetation cover, discontinuous in space (e.g. steppes) and/or in time (e.g. dry savannas). Soils are more exposed than in any other environment, as a result they are prone to erosion, particularly by wind. A second consequence is soils are an important component of the land surface viewed by satellite sensors, more and more dominant the dryer the climate. Whereas optical properties of vegetation are well studied and widely used in satellite monitoring of the biosphere (i.e. vegetation indices), soil surface features are less known and rarely monitored. In an attempt to fill this gap, this short review allows to distinguish biological and mineralogical characteristics. Soil color appears to be a major parameter of the drylands soils optical properties, as illustrated by examples in the Sahara. Previously explored causes of 'soil noise' in vegetation indices are confirmed as well as the way to correct it. Strategies for optimal use of optical remote sensing of drylands taking into account the soil surface are discussed in conclusion.

KEYWORDS: Optical remote sensing. Monitoring drylands. Soil color. Sahara. Vegetation indices.

Submission date: 05/04/2017
Acceptance date: 28/06/2017

1 INTRODUCTION

Drylands cover a large part of the world's landmass, encompassing a wide range of ecosystems, the vast steppes of Central Asia and North

[1] The Saharan part of this study has been made possible thanks to the contribution of Benoît Duchemin who collectected the soil samples in Libya and participated in the data analysis and interpretation.

[2] PhD in Earth Sciences/remote sensing, University Paris; Senior scientist. UMR Cesbio: CNRS-CNES-IRD-University of Toulouse, France. richard.escadafal@ird.fr

Africa; the Sahelian savannah and the Brazilian 'Caatinga' as well as real deserts such as the Sahara in Africa or the Gobi in China.

Drylands are defined as regions under a climate with average annual precipitation level (P) that is less than two- thirds of the evaporative capacity of the air (ETP, evapotranspiration) (ADEEL *et al*., 2005). Their climate is highly variable both in space and in time, even if these regions also experience seasons. .Each of the world's drylands has its own characteristics, but they have in common the irregularity of precipitation and the corresponding specific vegetation features discussed here in the context of remote sensing.

2 DRYLANDS OBSERVED BY SATELLITES

With regard to remote sensing, drylands have a decisive advantage: minimal cloud cover. This makes the use of optical imaging much easier, especially for observing and monitoring vegetation cover. The use of satellite images to study these vast areas, which are often difficult to observe directly on the ground, has appeared to be promising since the beginning of civilian remote sensing. Optical data are largely dominant in the catalogues of image providers, and widely used to monitor those areas[3].

2.1 DISCONTINUITY OF VEGETATION COVER

Whether the satellite sensor used to observe drylands is passive or active, the radiation that it receives is reflected or emitted by land surfaces primarily made up of soil and vegetation, with the latter generally being the less dominant element.

Classically, when optical remote sensing is used for ecological monitoring the emphasis is on monitoring green vegetation and is done mostly with the NDVI (normalized difference vegetation index). However as discussed below, the soil surface is most of the time the dominant component of drylands surfaces and their vegetation is often difficult to monitor with this standard approach (KENNEDY, 1989).

[3] A full chapter of the recent book entitled "Land Surface Remote Sensing: Environment and Risks", is dedicated to Drylands: Escadafal R. 2016, p. 1-23.

2.1.1 Discontinuity in time

In many drylands, the limited rainfall is occurring during a short rainy season, allowing the development of annual plants, fully covering the soil, like in dry savannas. This green cover will later become dead vegetation and litter, ultimately often disappearing and living the soil surface exposed. The vegetation cover is then discontinuous in time (see for example DARDEL *et al*., 2014).

2.1.2 Discontinuity in space

Figure 1 – Example of Drylands surfaces with discontinuous vegetation in clumps (bushes) exposing the soil (images from Google Earth)

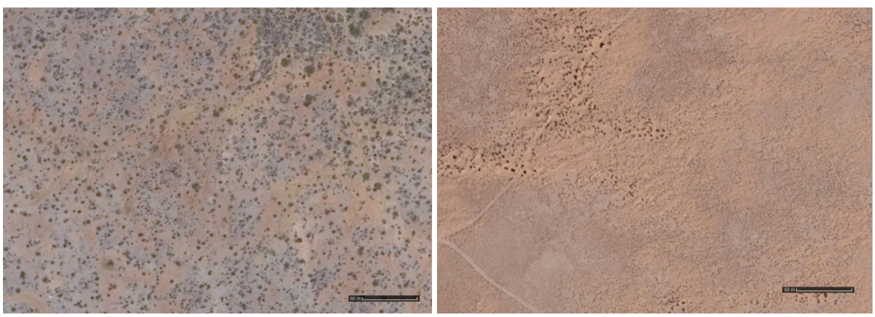

Note: Left : Belem de Sao Francisco, Pernambuco, Brazil (8.742°W 38.938°S,) 'open caatinga'; right: Bir Lahmar, South Tunisia (33.212°N 10.549°E), sandy steppe (rangeland).

In regions with steppic vegetation such as Northern Africa and the Middle East, and large parts of north and south American drylands, woody shrubs or perennial grasses form a sparse vegetation cover made of 'clumps'. The dryer the climate, the more spaced the plants, forming a discontinuous vegetation cover, where soil is also largely dominant (***figure 1***).

Another type of spatial discontinuity occurs when vegetation is organized into bands creates formations known as "tiger bush" in the Sahel. Field studies of the ecologic and hydrologic functioning of these environments have revealed that they represent an excellent adaptation to aridity (RIETKERK *et al*., 2004). It should also be noted that this type of organization in bands of vegetation separated by bands of bare ground is found, for example, in the traditional dry farming techniques on soft slopes in southern Tunisia (***Figure 2***).

Whether it follows identified patterns or not, the spatial distribution of vegetation on the soil surface has a strong impact on the water cycle. It determines this partition of the water and nutrients that it transports. Assessing it is a tool for a diagnosis of the state of ecological functioning.

Figure 2 – Example of Drylands surfaces with banded vegetation (images from Google Earth)

Note: Left: Kordofan,South Sudan (11.159 °N 28.279°E), natural 'tiger bush'; right: Belkhir, South Tunisia (39.387 °N 9.351°E), dryfarming cultivations

2.2 FEATURES OF THE SOIL SURFACE

Thus, because of the low level of precipitations and resulting minimal plant cover, soils are the major component of drylands surfaces. Weak primary production does not allow for a net enrichment of the soil in organic matter, so their content is generally low. They are most often exposed to precipitations causing water erosion, but wind erosion is also one of the major characteristics of drylands. Wind changes soils by removing of fine elements in some places and by accumulating sand in other locations. Moreover, wind combined with heat produces very intense evaporation, causing precipitation of solutes in the gaps in the soil, forming concretions, nodules and calcareous and/or gypseous crusts; sodium salts also precipitate in endorheic parts of the landscape.

Hence, soils in these regions are often sandy and poor in organic matter, and sometimes rich in carbonates, and they generally appear light when viewed from space. Eolian materials deposited in varying quantities (coatings, nebkhas, dunes, etc.) change the composition of the soil surface and can also change as a result of sandstorms. Sand trapped by vegetation forming continuous sandy veils is beneficial for the water balance of the ecosystem, as the favorish water infiltration and limit evaporation.

Other mineral components are coarser ones such as rocks, pebbles, stones and gravels. At the soil surface interesting biological components can also be found in the first millimetres: lichens and algae. With cyano-bacteria, mosses and other microorganisms they form ‘biocrusts’. Well-developed algal crusts are considered a diagnostic element of good health of the ecosystem (BELNAP; LANGE, 2001). With grasses, bushes and trees, these biocrusts compose the biological component varying with the climatic conditions and the seasons. When considering remote sensing, biological crusts are generally darkening the soil surface, and may produce a ‘photosynthetic’ signal, such as an increase of NDVI after rainy events (KARNIELI *et al*., 1999).

3 SPECTRAL FEATURES OF DRYLANDS USED IN REMOTE SENSING

3.1 VEGETATION INDICES

Monitoring vegetation is one of the most widely used applications of civilian remote sensing, particularly through the uses of various ‘vegetation indices’. This concept is based on the contrast between the reflectance properties of green plants in the red and near infrared (NIR) spectral domain. For instance, the Normalised Difference Vegetation Index (NDVI) is defined as the ratio of the difference to the sum between red and NIR reflectances (TUCKER, 1979). The success of the NDVI relies on its simplicity as it uses only the two spectral bands most widely available, and on a certain robustness relative to directional and atmospheric effets (HOLBEN, 1986). NDVI imagery is routinely available from the main global monitoring satellite systems, i.e. the American NOAA-AVHRR and NASA-MODIS (JUSTICE *et al*., 1998) and the European SPOT-VEGETATION programmes (MAISONGRANDE *et al*., 2004). Green vegetation in drylands is easily monitored when its density is similar to the one of less dry areas, as it happens during the rainy season or in irrigated areas, e.g. However, numerous studies have shown the limitations of the NDVI approach particularly for low values, low green vegetation densities are poorly detected, and NDVI imagery can be affected by soil background noise as we discuss now.

3.2 SOILS OPTICAL PROPERTIES

3.2.1 Soils in the visible domain: their color

Whereas soil color is a parameter well used since the beginning of Soil Science, its consideration in remote sensing is rather limited. Despite color is fundamentally a human sensation, it has been demonstrated it is strictly related to spectral reflectance, and the corresponding optical laws are the subject of Color Science, also known as colorimetry, described in voluminous treatises (see WYSZECKI; STILES, 2000).

In brief, the color of an object depends on its reflective properties in the 370-770 nm, gamut of the human eye sensitivity. From its spectral reflectance measured in this range, it is possible to compute and predict the color of this object, for a 'standard observer'.

This evidently applies also to soils, and modern equipments such as spectrocolorimeters allow to determine soil color with high precision, in various color systems. However, the usual way color is determined by soil scientist is the well established method of comparison with color tables. Special color tables have been designed by the Munsell Company and the soil science societies recommend to record soil color using the Munsell notation, particularly during field surveys (ESCADAFAL *et al*., 1988).

Notably, among the laws of colorimetry, a specific one called metamerism states that is not possible to obtain the spectral reflectance of an object from its color notation, because different reflectance spectra can produce the same color sensation. But in the case of soils, it has been shown that is possible to predict reflectance in the visible bands from the Munsell color, when soils have a monotonous spectral reflectance curve, which is the case for a large number of soils (ESCADAFAL *et al*., 1989). As an example, red desert soils will have all a similar reflectance curve, with a strong absorption in the blue region (see case study).

3.2.2 Soils reflectance in the near infrared and 'soil noise'

Whereas the strong reflection of solar radiation by green vegetation in the near-infrared has been amply studied, soil properties in this domain have been initially considered as rather neutral and invariable. The design of vegetation index such as the NDVI rely on the concept of 'soil line' that is to say of an invariant Vis/NIR ratio, as further explained in the case study.

But some of the early users of AVHRR imagery over the desert part of Africa had noticed local variations of the NDVI apparently unrelated to differences in vegetation cover, called ‘desert artefacts’ (HUETE; TUCKER, 1991). These permanent NDVI features cannot be related to permanent vegetation communities as none is to be found in those barren areas. These fluctuations of NDVI values in the 0 to 0.2 range seem essentially related to geomorphic features (LE HOUÉROU, 1986), and thus to the spectral properties of desert land surfaces. As an example in Mediterranean rangelands studied in Syria, bare soil surfaces show NDVI values fluctuating in the 0 to 0.18 range (EVANS; GEERKEN, 2004). Similarly in a monitoring experiment of the arid zone of Jordan

Figure 3 – Location of the studied desert soil samples in the Sahara

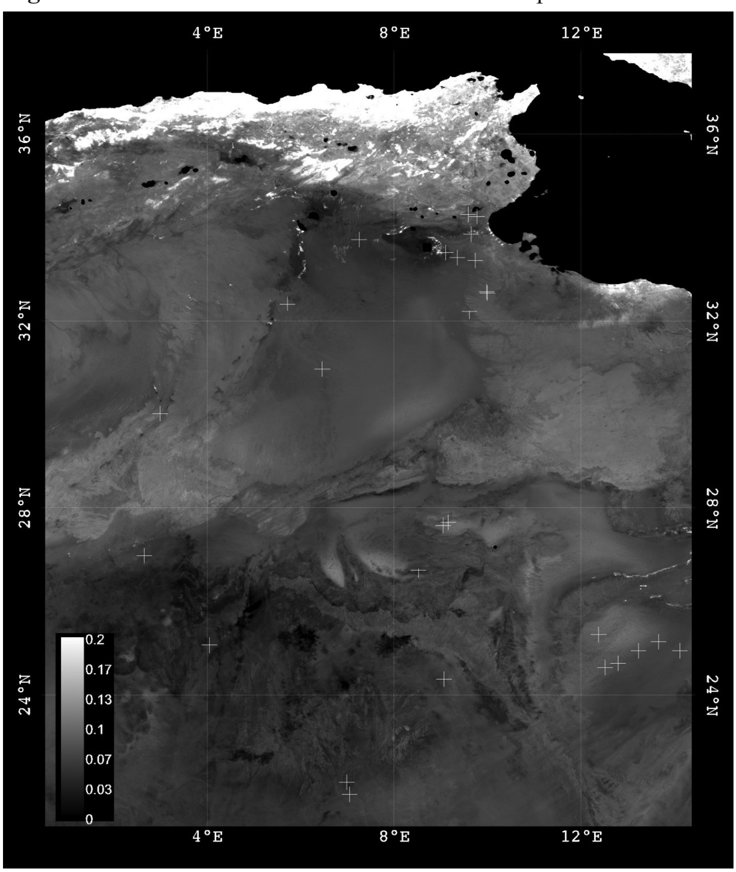

Note: Background image is a SPOT-VGT NDVI composite (1st decade of July 2003) showing ‘soil noise’; grey level values are stretched between 0 and 0.2 (see scale) with AVHRR, NDVI values were found to vary between 0.05 and 0.12 (AL-BAKRI; TAYLOR, 2003). The fluctuations of the NDVI values over the Sahara displayed in ***figure 3*** are exactly of the same nature, illustrating the concept of soil noise.

This creates difficulties to discriminate low covering vegetation (JIANG *et al*., 2008). Indeed, the variation of the NDVI over these artefacts is in the same magnitude as those to be detected to monitor plant growth in drylands. Because of this inability of NDVI to discriminate vegetation covers in the 0-20% range (ISHIYAMA *et al*., 2001), it fails at monitoring efficiently desertification in semi-arid areas (BAI *et al*., 2008).

Since soil influence in NDVI has been recognised, several solutions have been developed to dampen it. The main strategy has been targeting the adjustment to the real soil line, which usually does not cross the Red/NIR axes at the origin. Based on these observations, the Soil Adjusted Vegetation Index (SAVI) has been designed, taking also into account the fact that the vegetation isolines are not parallel to the soil line (HUETE, 1988).

Numerous refinements and variations have been derived from this successful approach. However, all these are two-band vegetation indices mainly designed to be used with AVHRR sensor. As an extent of two-band VIs, several authors have looked at ways to take advantage of the enhanced capacities of new low resolution satellites with more channels in the visible domain. In particular, the blue band has attracted interest in attempts to take account for the atmospheric effects. These are indeed stronger in the shorter wavelengths, and indices have been formulated to use the blue band to reduce the atmospheric effects on the Red/NIR ratio, such as the atmospherically resistant vegetation index, ARVI (KAUFMAN; TANRE, 1992) and SARVI its adaptation using the SAVI approach (HUETE *et al*., 1997). However, these 3-bands vegetation indices were designed for rather densely vegetated areas, and found to be very sensitive to soil background (HUETE; LIU, 1994).

4 CASE STUDY: spectral properties of selected desert soils

4.1 COLLECTION OF DESERT SOILS SAMPLES IN THE SAHARA

As the “desert artefacts” have been first recognised in the Sahara, a selection of surface samples has been gathered from several spots in this desert, representing a variety of situations.

The area investigated is among the less accessible in the world as it lies in the heart of the Sahara only reachable by off-road exploration. The sample collection assembled for this study has benefited from field work in Tunisia, plus two expeditions to the Saharan ergs, one made in Algeria, the other one in Libya (see ***figure 3***). Due to limited carrying capacity, the sampling has been designed to cover the largest range of type of surface material, without possibly pretending to be systematic. Each of the thirty samples gathered has been obtained by collecting about 1kg from horizontal not hardened surfaces, at a depth of 0-5 cm. They have been chosen to represent as much as possible the variety of sandy and gravelly surface types over the Saharan desert (***table 1***).

Table 1 – Reflectance values of the studied samples in the spectral bands of SPOT-VGT sensor

Site	Location		Type of surface	Average values			
Number	Lon E (deg)	Lat N (deg)		Blue	Red	NIR	NDVI
1	34.275	9.587	Loamy soil	0.191	0.471	0.535	0.064
2	34.230	9.768	Loamy soil	0.168	0.431	0.494	0.068
3	32.62	9.980	Sandy loamy	0.138	0.372	0.428	0.070
4	32.205	9.609	Sandy soil	0.160	0.433	0.500	0.072
5	32.594	9.995	Sand accumulation	0.147	0.385	0.447	0.074
6	33.294	9.736	Sandy hummock	0.093	0.319	0.379	0.086
7	34.230	9.768	Sand veil	0.178	0.499	0.572	0.067
8	33.457	9.100	Sandy surface	0.234	0.520	0.578	0.053
9	33.849	9.648	Gypsiferous sand	0.278	0.510	0.550	0.038
10	32.619	9.980	Sandy loam	0.202	0.482	0.533	0.051
11	30.969	6.464	Gravelly	0.116	0.366	0.430	0.081
12	27.691	9.159	Very reddish sand dune	0.056	0.268	0.336	0.113
13	27.619	9.053	Reddish sand dune	0.073	0.336	0.411	0.101
14	24.333	9.067	Coarse sand	0.071	0.333	0.401	0.093
15	22.133	6.983	Fine sand	0.152	0.396	0.451	0.065

16	21.867	7.050	Sandy surface	0.101	0.361	0.424	0.080
17	25.063	4.053	Gravelly surface	0.134	0.395	0.459	0.075
18	26.977	2.660	Coarse sand	0.154	0.354	0.403	0.064
19	30.017	2.992	Fine reddish sand	0.124	0.301	0.342	0.064
20	32.349	5.716	Fine sand	0.112	0.299	0.349	0.078
21	33.733	7.250	Bright sand surface	0.110	0.317	0.370	0.078
22	26.664	8.522	Fine sand	0.213	0.420	0.469	0.055
23	25.292	12.375	Very reddish sand	0.077	0.359	0.435	0.096
24	24.940	14.109	Sand dune	0.132	0.411	0.474	0.071
25	25.138	13.658	Sand dune	0.159	0.448	0.513	0.068
26	24.945	13.226	Sand dune	0.128	0.439	0.510	0.075
27	24.678	12.789	Sand dune	0.154	0.437	0.497	0.064
28	24.678	12.789	Sand dune	0.156	0.430	0.488	0.063
29	24.584	12.515	Sand dune	0.121	0.398	0.460	0.072
30	33.352	9.352	Fine sand	0.217	0.462	0.511	0.050

Source: Made by the authors

The spectral reflectance properties of the desert material samples have been measured using a field portable spectroradiometer covering the 400-2400 nm range (Fieldspec Pro from Analytical Spectral Devices). Air-dried sample have been placed in circular glass plates of 20 cm diameter, forming a levelled layer about 2cm thick. The fiber optic sensor having a field of view of 15° was placed 20 cm above the sample surface maintained horizontally. Measurements have been performed outdoors, under direct sun illumination with clear sky condition. Measurement times were chosen to keep the sun elevation angles within the 50-70°range, and with the instrument sensor viewing angle at nadir. Values of spectral radiance reflected by each sample have been ratioed by the incoming radiation measured over a calibration panel made of 100% reflective polytetrafluoroethylene (Spectralon).

In relation to the satellite sensors considered in this study only the reflectance values in the VIS-NIR domain are used. Continuous reflectance spectra have been converted into discrete values, by convolution with the characteristics of transmission filters of VIS-NIR spectral bands of NOAA-AVHRR and SPOT-VEGETATION (VGT) sensors, to allow comparison with remotely sensed data (LILLESAND et al., 2014). As results for the two sensors are extremely similar, those of SPOT-VGT have been used in the rest of this study. ***Table 1*** displays reflectance values obtained in SPOT-VGT bands for the 30 desert soil samples studied.

4.2 TYPICAL DESERT SOIL SPECTRAL SIGNATURES

Average reflectance spectra obtained with 10 repetitions per sample are illustrated on ***figure 4*** through five typical spectra selected among the whole set of samples described in ***Table 1***.

The sigmoïdal shape is due to the absorption in the shorter wavelength, which is the strongest in the case of the 'very reddish sand' (sample#12). On the opposite the 'gypsiferous sand' (sample#9) shows a less pronounced shape and is the brightest sample (higher average reflectance, or albedo). Finally 'coarse sand' (sample#18) is the darkest, giving an idea of the range of spectra observed for desert soils.

Figure 4 – Example of reflectance spectra obtained for the studied desert soils. Five samples show the variation range in the blue to NIR spectral domain

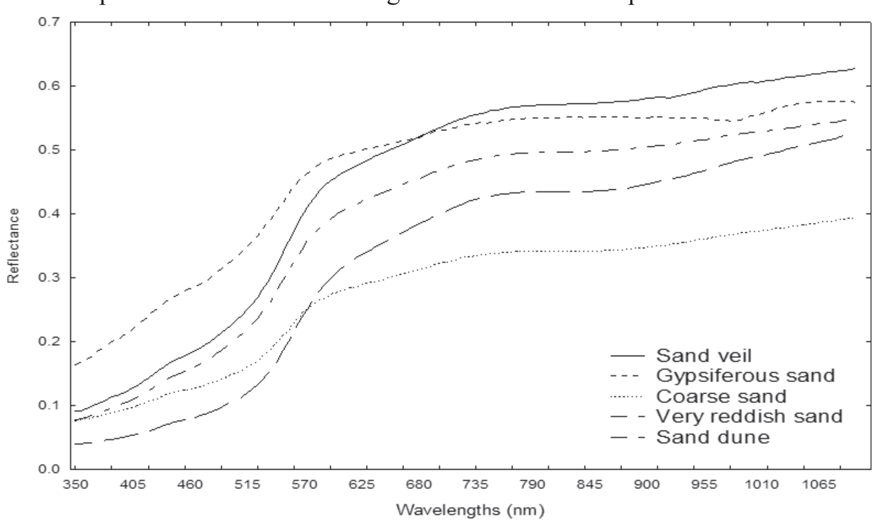

4.3 EVIDENCE OF THE SOIL LINE CONCEPT AND IMPACT ON NDVI

Measured reflectances in the sensor bands displayed in the red/NIR scattergram of ***figure 5*** show the distribution of the desert samples along a line. Values shows large differences in surface brightness, but the points are not on the 1:1 line which is at the basis of the soil line concept (BARET *et al*., 1993).

Indeed points do not align perfectly, as they do not show exactly the same red/nir ratio. This is consistent with earlier observations on desert soils of Nevada, (e.g. ELVIDGE; LYON ,1985). Because the NDVI formulation assumes all soils have the same constant red/NIR ratio, departure from the 1:1 line is responsible for differences in NDVI values. The analysis of ***table 1*** shows that the NDVI varies here from 0.038 to 0.113 for those bare desert soils.

Another feature of the soil line in ***figure 5*** is the dispersion along the second axis (orthogonal to the main elongation axis), leading to consider that the soil line has a certain thickness. In order to analyse the origin of the dispersion of the soil samples in the Red/NIR space, we hypothesise that the Red/NIR is not independent of the absorption features found in the visible bands, as already found while studying other soil samples (ESCADAFAL; HUETE, 1991). One of the most frequent features of desert soils is the presence of iron oxide coatings on sand grains, responsible for light absorption in the blue band, resulting in their reddish colour (BEN-DOR *et al*., 2006; ESCADAFAL, 1994). These features impact the general shape of the reflectance curve and are responsible for the non constant Red/NIR ratio.

Figure 5 – The 30 desert soil samples define a specific soil line in the Red/NIR plane. This line does not cross the origin, and points are dispersed around it, these are the two causes of soil noise in the NDVI, data from ***table 1***.

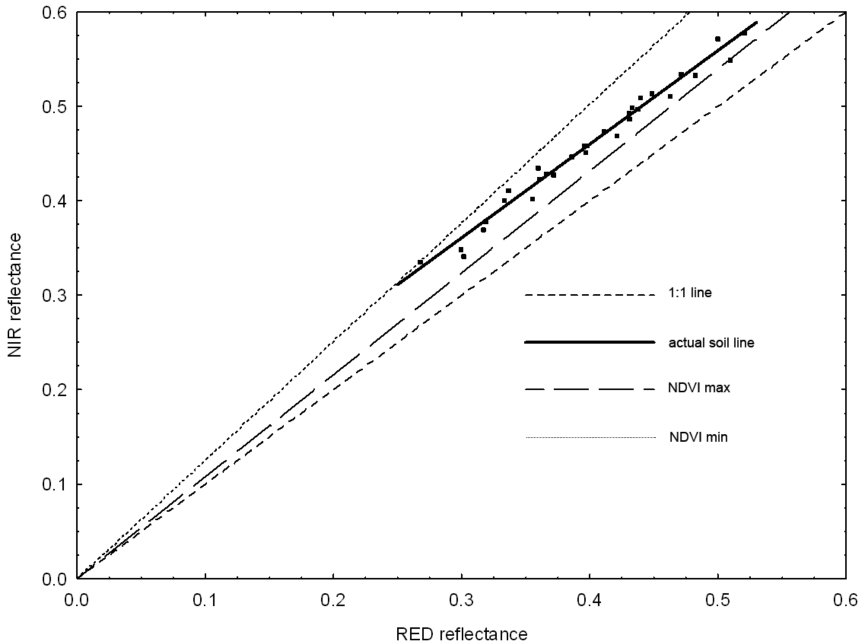

4.4 CORRECTION VEGETATION INDICES FOR SOIL NOISE

The correlation between reflectances in the blue, red and NIR bands appears on ***figure 6*** plotting values for the 30 samples in the space of these 3 bands. This reveals that the desert soils are located on a 'soil plane' rather than a soil line. As this plane is not strictly orthogonal to the Red/NIR one, when viewing the points in those two dimensions, they appear with some dispersion, this explains the soil line 'thickness'.

Figure 6 – Desert soil samples in the Blue/Red/NIR space depict a 'soil plane'

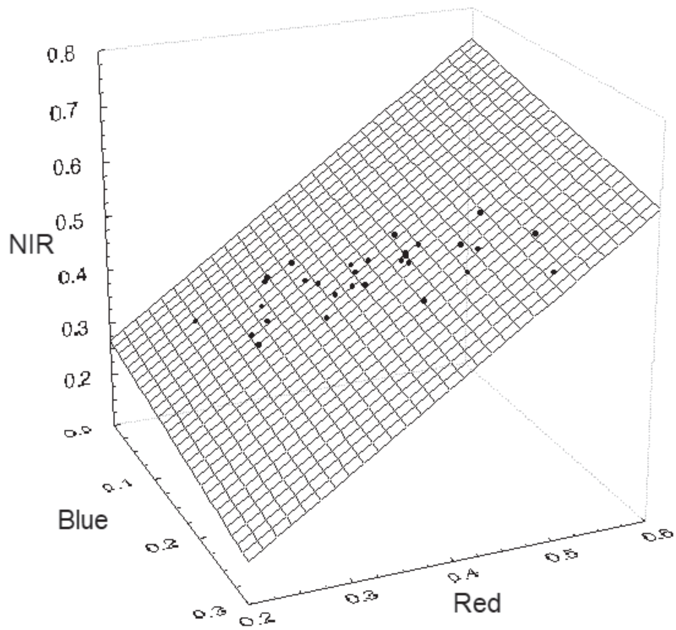

Note: Viewed from the NIR/Red face (such as in ***figure 3***), this 3D scattergramms explains the origin of the soil line 'thickness' as the soil plane is not orthogonal to this face.

This result allows considering different options to take this specific distribution of the desert soil values into account to minimise the soil noise. A simple approach is to use the above results to correct reflectance by acknowledging the Red/NIR contrast is correlated to the Red/Blue ratio. That is to say, the relative decrease of reflectance in the Red band depends on the intensity of the absorption in the Blue band. Contrasts between bands are easily expressed by the normalised difference between them. Then, a first simple formulation is to subtract from the NDVI a noise fraction k of the redness index, RI (ESCADAFAL *et al*., 1989). This index is a normalised difference between the red and blue bands, and the noise fraction is estimated using the slope k of the NDVI/RI correlation (ESCADAFAL; HUETE, 1991) as illustrated on ***figure 7*** for the present data set.

Figure 7 – Correlation between the NDVI (NIR/Red normalised difference) and IC, Redness Index (Red/blue normalised difference) used to correct for soil noise (NDVI* approach)

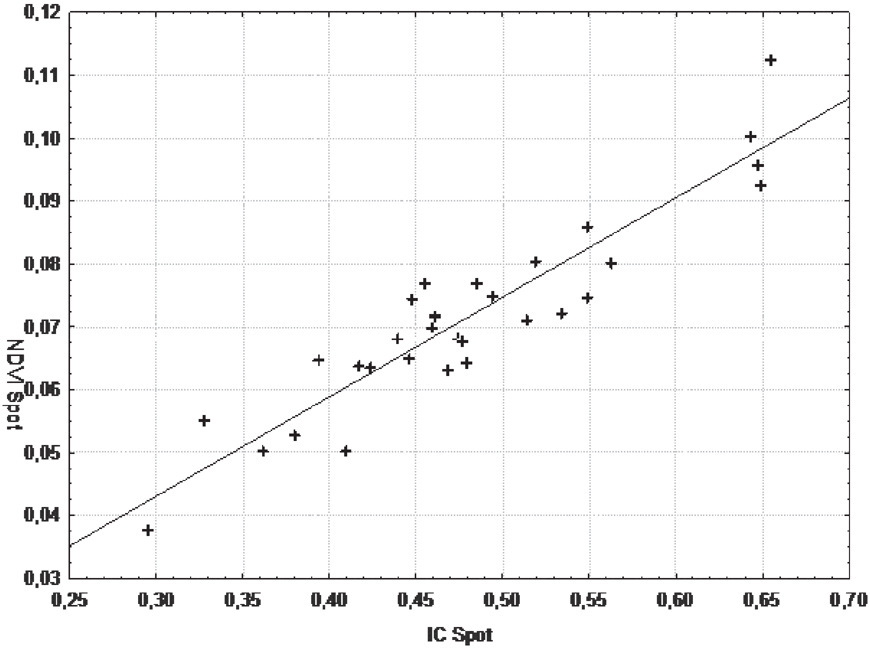

Note: y = – 0.0044 + 0.158 x / r2 = 0.861

The vegetation index corrected for soil noise is then noted NDVI*, where $NDVI^{*} = \frac{\rho_{nir} - \rho_{r}}{\rho_{nir} + \rho_{r}} - k \times \frac{\rho_{r} - \rho_{b}}{\rho_{r} + \rho_{b}}$ (ESCADAFAL; HUETE 1991) where ρ_b, ρ_r, ρ_{nir} are the reflectance value in the blue, red and NIR bands, respectively. In the case of our dataset the value found for *k* is 0.158. This value is likely to vary slightly for different sensors, but the approach initiated in the previous work cited has proven to be applicable here to the desert soils of the Sahara.

5 CONCLUSION: consequences for the use of Earth Observation in Drylands

This short review of the role of soils in remote sensing of drylands has come to the conclusions that soils and their surface features are a major component of the land surface of those regions and are often largely dominant. While using remote sensing for monitoring, such as in international programs to combat desertification, emphasis is classically put on assessing the trends in green vegetation cover changes. In this study we have evidenced the influence of desert soils on the vegetation indices (soil noise) and validated the principle of its correction. Other options such as computing a distance to the 'soil plane' would allow to refine 'desert adjusted' vegetation indices. Taking into account this particularity of drylands by applying the correction to actual imagery should improve the detection of low green vegetation covers in those vast regions.

Moreover some symptoms of land degradation (and recovery) might rather to be observed on the mineral component of the land surface, such as changes in the distribution of Aeolian deposits, traces of salt deposition, changes in color related to exposure of different soil layers following erosion, e.g. As a conclusion it can be advocated that when using optical remote sensing for drylands, soils are definitely in the picture.

REFERENCES

ADEEL, Z. *et al*., ***Ecosystems and Human Well- being: Synthesis***. Millennium Ecosystem Assessment. Washington, DC, World Resources Institute, 2005. p. 155.

AL-BAKRI, J. T.; TAYLOR, J. C. Application of NOAA AVHRR for monitoring vegetation conditions and biomass in Jordan. ***Journal of Arid Environments***, v. 54, n. 3, p. 579-593, 2003.

BAI, Z. G., DENT, D. L., OLSSON, L. & SCHAEPMAN, M. E. Proxy global assessment of land degradation. ***Soil Use and Management***, v. 24, n. 3, p. 223-234, 2008.

BARET, F.; JACQUEMOUD, S.; HANOCQ, J. F. The soil line concept in remote sensing. ***Remote Sensing Reviews***, v. 7, n. 1, p. 65-82, 1993.

BELNAP, J.; LANGE O. L. ***Biological Soil Crusts: Structure, Function, and Management***. Springer, Berlin, 2001.

BEN-DOR, E. *et al*. Quantitative mapping of the soil rubification process on sand dunes using an airborne hyperspectral sensor. ***Geoderma***, v. 131, n. 1, p. 1-21, 2006.

DARDEL, C. *et al*. Re-greening Sahel: 30years of remote sensing data and field observations (Mali, Niger). ***Remote Sensing of Environment***, v. 140, p. 350-364, 2014.

ELVIDGE, Christopher D.; LYON, Ronald JP. Influence of rock-soil spectral variation on the assessment of green biomass. ***Remote Sensing of Environment***, v. 17, n. 3, p. 265-279, 1985.

ESCADAFAL, R.; GIRARD, M. C.; COURAULT, D. "Modeling the relationships between Munsell soil color and soil spectral properties", ***International Agrophysics***, v. 4, n. 3, p. 249-261, 1988.

ESCADAFAL, R.; GIRARD, M. C.; COURAULT, D. Munsell soil color and soil reflectance in the visible spectral bands of Landsat MSS and TM data. ***Remote Sensing of Environment***, v. 27, n. 1, p. 37-46, 1989.

______________; HUETE, A. Improvement in remote sensing of low vegetation cover in arid regions by correcting vegetation indices for soil ''noise''. ***Comptes Rendus de l'***, v. 312, n. 11, p. 1385-1391, 1991.

______________; Soil spectral properties and their relationships with environmental parameters-examples from arid regions. In: ***Imaging Spectrometry—a Tool for Environmental Observations.*** Springer Netherlands, 1994. p. 71-87.

______________. Drylands and desertification. In: ***Baghdad N; Zribi M.,eds. Land Surface Remote Sensing: Environment and Risks***, 1st edition (London: Oxford: ISTE Press – Elsevier), 2016. p.1-23.

EVANS, J.; GEERKEN, R. Discrimination between climate and human-induced dryland degradation. ***Journal of Arid Environments***, v. 57, n. 4, p. 535-554, 2004.

HOLBEN, B. N. Characteristics of maximum-value composite images from temporal AVHRR data. ***International journal of remote sensing***, v. 7, n. 11, p. 1417-1434, 1986.

HUETE, A. R. A soil-adjusted vegetation index (SAVI). ***Remote sensing of environment***, v. 25, n. 3, p. 295-309, 1988.

___________; TUCKER, C. J. Investigation of soil influences in AVHRR red and near-infrared vegetation index imagery. ***International Journal of Remote Sensing***, v. 12, n. 6, p. 1223-1242, 1991.

___________; LIU, H. Q. An error and sensitivity analysis of the atmospheric-and soil-correcting variants of the NDVI for the MODIS-EOS. ***IEEE Transactions on Geoscience and Remote Sensing***, v. 32, n. 4, p. 897-905, 1994.

___________; LIU, H. Q. , BATCHILY K.,VAN LEEUWEN W.(1997). "A comparison of vegetation indices over a global set of TM images for EOS-MODIS." Remote Sensing of Environment 59: 440-451, 1997.

JIANG, Zhangyan *et al*. Development of a two-band enhanced vegetation index without a blue band. ***Remote Sensing of Environment***, v. 112, n. 10, p. 3833-3845, 2008.

JUSTICE, C. O., *et al*. The Moderate Resolution Imaging Spectroradiometer (MODIS): Land remote sensing for global change research. ***IEEE transactions on geoscience and remote sensing,*** v. 36 n. 4, p. 1228-1249, 1988.

KARNIELI, Arnon *et al*. Spectral characteristics of cyanobacteria soil crust in semiarid environments. ***Remote Sensing of Environment***, v. 69, n. 1, p. 67-75, 1999.

KAUFMAN, Y. J.; TANRE, D. Atmospherically resistant vegetation index (ARVI) for EOS-MODIS. ***IEEE transactions on Geoscience and Remote Sensing***, v. 30, n. 2, p. 261-270, 1992.

KENNEDY P. J. Monitoring the phenology of Tunisian grazing lands. ***International Journal of Remote Sensing***, v. 10, n. 4-5, p. 835-845, 1989.

LE HOUÉROU, H. N. The desert and arid zones of northern Africa. In: ***Hot deserts and arid shrublands*** (ed. I. N.-M. a. D. W. G. M. Evenari). Amsterdam: Elsevier, 1986. p. 101-147.

LILLESAND, P. T. M. & KIEFER, R. W. CHIPMAN W. ***Remote Sensing and Image Interpretation***. John Wiley & Sons, 2014.

MAISONGRANDE, P.; DUCHEMIN, B.; DEDIEU, G. VEGETATION/SPOT: an operational mission for the Earth monitoring; presentation of new standard products. ***International Journal of Remote Sensing***, v. 25, n. 1, p. 9-14, 2004.

RIETKERK, M. *et al*. Self-organized patchiness and catastrophic shifts in ecosystems. ***Science***, v. 305, n. 5692, p. 1926-1929, 2004.

SHIYAMA, T. *et al*. Relationship among vegetation variables and vegetation features of arid lands derived from satellite data. ***Advances in Space Research***, v. 28, n. 1, p. 183-188, 2001.

TUCKER, Compton J. Red and photographic infrared linear combinations for monitoring vegetation. ***Remote sensing of Environment***, v. 8, n. 2, p. 127-150, 1979.

WYSZECKI, G. and W. S. STILES. ***Color science: concepts and methods, quantitative data, and formulae***. John Wiley & Sons, 2000.